

BARYONIC SPIN HALL EFFECTS IN Au+Au COLLISIONS AT $\sqrt{s_{NN}} = 7.7\text{--}200$ GeV*

BAOCHI FU^{a,b,c}, LONGGANG PANG^d, HUICHAO SONG^{a,b,c}, YI YIN^{e,f}

^aCenter for High Energy Physics, Peking University, Beijing 100871, China

^bDepartment of Physics & State Key Laboratory of Nuclear Physics
and Technology, Peking University, Beijing 100871, China

^cCollaborative Innovation Center of Quantum Matter, Beijing 100871, China

^dKey Laboratory of Quark & Lepton Physics (MOE)
and Institute of Particle Physics, Central China Normal University
Wuhan 430079, China

^eQuark Matter Research Center, Institute of Modern Physics
Chinese Academy of Sciences, Lanzhou 730000, China

^fUniversity of Chinese Academy of Sciences, Beijing 100049, China

*Received 1 August 2022, accepted 29 August 2022,
published online 14 December 2022*

In these proceedings, we present our recent prediction on the local net Lambda polarization to search for the baryonic spin Hall effect (SHE) at RHIC BES energies. The baryonic SHE is induced by the gradients of baryon chemical potential, which leads to local polarization separation between baryons and anti-baryons. Based on hydrodynamic simulations with the spin Cooper–Fryer formula, we propose to use $P_{2,y}^{\text{net}}$ and $P_{2,z}^{\text{net}}$, the second Fourier coefficients of net spin polarization to quantify this baryonic SHE. Future experimental observation of their non-trivial signatures could strongly support the existence of the baryon SHE in hot and dense QCD matter.

DOI:10.5506/APhysPolBSupp.16.1-A40

1. Introduction

In relativistic heavy-ion collisions, the produced quark–gluon plasma (QGP) carries a large amount of orbital angular momentum, which induces the spin polarization of quarks and final hadrons through the spin-orbital coupling [1, 2]. Within the hydrodynamic approach with equilibrium assumption, the thermal vorticity developed during the system evolution leads to the hyperon spin polarization at the freeze-out surface described by the

* Presented at the 29th International Conference on Ultrarelativistic Nucleus–Nucleus Collisions: Quark Matter 2022, Kraków, Poland, 4–10 April, 2022.

spin Cooper–Frye formula [3]. The related model calculations successfully describe the global Λ polarization but fail to reproduce its azimuthal angle dependence, which is known as the “local spin polarization puzzle” [4–7]. Recently, it was found that, besides the widely studied thermal vorticity effect, the spin polarization can also be induced by the shear stress tensor [8–11]. Hydrodynamic simulations demonstrate that such shear-induced polarization (SIP) is always opposite to the thermal vorticity effect and could lead to the right sign of local polarization as experimental data in some certain freeze-out conditions [9, 11].

If we focus on the collisions at RHIC BES energies, another spin polarization mechanism induced by the gradient of baryon chemical potential ($\nabla\mu_B$ -IP) becomes relevant. Such an effect is also called the baryonic spin Hall effect, which can be derived from the quantum kinetic theory [8, 12–16], but has not been fully explored phenomenally. In these proceedings, we will briefly introduce our recent prediction on the second Fourier coefficients of net spin polarization to search for the baryonic spin Hall effect (SHE) at RHIC BES energies. For more details, see our recent works [9, 17].

2. Method

In a many-body system of fermions, the spin polarization vector is described by the axial Wigner function $\mathcal{A}^\mu(x, p)$. To the first order, \mathcal{A}^μ can be expressed by the gradients of temperature T , flow velocity u^μ , and baryon chemical potential μ_B [8, 18] (see also Refs. [14, 16])

$$\begin{aligned} \mathcal{A}^\mu(x, p) = & \beta f_0(x, p)(1 - f_0(x, p))\varepsilon^{\mu\nu\alpha\rho} \\ & \times \left(\underbrace{\frac{1}{2}p_\nu\partial_\alpha^\perp u_\rho}_{\text{vorticity}} - \underbrace{\frac{1}{T}u_\nu p_\alpha\partial_\rho T}_{\text{T-gradient}} - \underbrace{\frac{p_\perp^2}{\varepsilon_0}u_\nu Q_\alpha^\lambda\sigma_{\rho\lambda}}_{\text{SIP}} - \underbrace{\frac{q_B}{\varepsilon_0\beta}u_\nu p_\alpha\partial_\rho(\beta\mu_B)}_{\text{baryonic SHE}} \right), \end{aligned} \quad (1)$$

where $f_0(x, p) = (e^{(\varepsilon_0 - q_B\mu_B)\beta} + 1)^{-1}$ is the Fermi–Dirac distribution function with $\varepsilon_0 = p \cdot u$, q_B is the baryon number, and $\beta = 1/T$ is the inverse temperature. Here, the transverse projection is defined as $\partial_\perp^\mu \equiv \Delta^{\mu\nu}\partial_\nu$ and $p_\perp^\mu \equiv \Delta^{\mu\nu}p_\nu$ with $\Delta^{\mu\nu} = g^{\mu\nu} - u^\mu u^\nu$. After combining the first two terms with the ideal hydrodynamic equation $(u \cdot \partial)u_\alpha = -\beta^{-1}\partial_\alpha^\perp\beta + \mathcal{O}(\partial^2)$, we will get the widely known “thermal vorticity” term $\frac{1}{2\beta}p_\nu\partial_\alpha(\beta u_\rho)$.

The third term of Eq. (1) denotes the shear-induced polarization, where the generalized momentum quadrupole tensor and shear stress tensor are defined as $Q^{\mu\nu} = -p_\perp^\mu p_\perp^\nu / p_\perp^2 + \Delta^{\mu\nu}/3$ and $\sigma^{\mu\nu} = \partial_\perp^{(\mu} u^{\nu)} - (1/3)\Delta^{\mu\nu}(\partial \cdot u)$. This expression can be obtained from chiral kinetic theory or linear response theory [8, 9]. In [10, 11], the statistical method also gives a similar form. Such

a shear term induces similar differential polarization $P_z(\phi)$ and $P_y(\phi)$ [9, 11] as observed in experiment, which is essential to solve the “local spin polarization puzzle”, see [16, 19–22] for recent developments in the phenomenological study. The last term of Eq. (1) is the baryon spin Hall effect (SHE), which is induced by the gradients of baryon chemical potential and becomes significant at RHIC BES energies.

To calculate the differential Λ spin polarization $P^\mu(p)$, we employ the “spin Cooper–Frye” formula that averages $\mathcal{A}^\mu(x, p)$ over the freeze-out hypersurface

$$P^\mu(\mathbf{p}) = \frac{\int d\Sigma^\alpha p_\alpha \mathcal{A}^\mu(x, \mathbf{p}; m)}{2m \int d\Sigma^\alpha p_\alpha f_0(x, p)}. \quad (2)$$

Here, we consider two scenarios — “Lambda equilibrium” and “strange memory” for the spin polarization at freeze-out, which correspond to two extreme conditions of the spin relaxation time during hadronic evolution [1, 3, 9]. In the model calculation, we set $m = 1.116$ GeV, $q_B = \pm 1$ for the “Lambda equilibrium” scenario, and $m = 0.3$ GeV, $q_B = \pm 1/3$ in Eq. (2) for the “strange memory” scenario, respectively.

3. Results and discussions

In this work, we implement 3+1-d hydrodynamics MUSIC with AMPT initial conditions [23–25] to simulate Au+Au collisions at $\sqrt{s_{NN}} = 7.7$ –200 GeV. The spin Cooper–Frye formula (Eq. (2)) is implemented on the hyper-surface with constant energy density, which roughly matches the chemical freeze-out temperature from the statistical model. For more details of the model and parameter set-ups, please refer to [5].

Figure 1 shows the contributions from the vorticity, T -gradient, shear, and baryonic SHE to the differential spin polarization in Au+Au collisions at $\sqrt{s_{NN}} = 7.7$ GeV. Analogous to the results of high-energy collisions [9, 11, 16], the shape of $P_z(\phi)$ and $P_y(\phi)$ is mostly determined by the competition between the T -gradient and SIP effects. In the strange memory scenario, the SIP becomes more important due to the smaller mass of the spin carrier. On the other hand, with the large chemical potential, the baryonic SHE shows a significant contribution to differential polarization, especially for $P_z(\phi)$ in both scenarios at 7.7 GeV. For baryons and anti-baryons, since the sign of the baryonic SHE is opposite, a sizeable separation between their differential polarization is anticipated [17].

To characterize this separation and probe the baryon SHE signal, we construct the second harmonic component of polarization for the net lambda/strangeness

$$P_{2,z}^{\text{net}} \equiv \langle P_z^{\text{net}}(\phi) \sin 2\phi \rangle, \quad P_{2,y}^{\text{net}} \equiv -\langle P_y^{\text{net}}(\phi) \cos 2\phi \rangle, \quad (3)$$

where $P_{z,y}^{\text{net}}(\phi) \equiv P_{z,y}(\phi) - \bar{P}_{z,y}(\phi)$ denotes the net spin polarization with $P_{z,y}(\phi)$ and $\bar{P}_{z,y}(\phi)$ denotes the differential polarization along the longitudinal direction (z) and out-of-plane direction (y) for baryons and anti-baryons, respectively. Here, $\langle \dots \rangle$ is the average over the azimuthal angle. Figure 2 shows $P_{2,z}^{\text{net}}$ and $P_{2,y}^{\text{net}}$ in Lambda equilibrium and strange memory scenario.

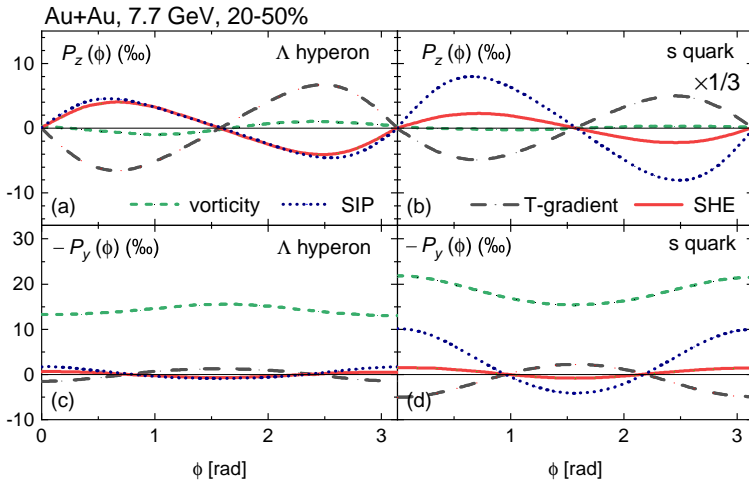


Fig. 1. (Color on-line) Differential spin polarization $P_z(\phi)$ and $-P_y(\phi)$ in 7.7 GeV Au+Au collisions from Lambda equilibrium scenario and strange memory scenario, respectively. The colored curves show the contributions from the vorticity, T-gradient, shear, and baryonic SHE.

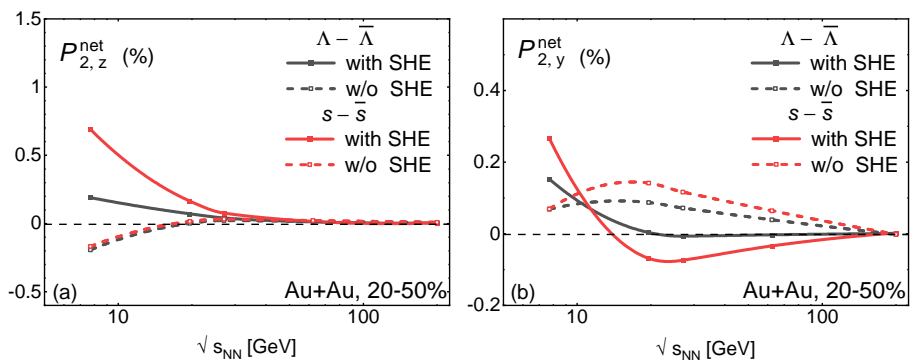


Fig. 2. The second Fourier coefficients of net spin polarization, $P_{2,z}^{\text{net}}$ and $P_{2,y}^{\text{net}}$ as a function of collision energy in Lambda equilibrium and strange memory scenarios.

When including SHE, the longitudinal component $P_{2,z}^{\text{net}}$ increases with the decrease of collision energy, corresponding to the increasing separation between $P_z(\phi)$ and $\bar{P}_z(\phi)$. On the other hand, $P_{2,y}^{\text{net}}$ shows an interesting non-monotonic dependence with the collision energy, which is insensitive to the choice of scenario. Such non-trivial energy dependence is related to the net baryon density distribution correspondingly: $n_B(x, y)$ in the transverse plane shows a similar almond shape in all energies, while its reaction plane profile $n_B(x, \eta_s)$ shows different peak structure from baryon stopping. See our discussion in [17] for details.

4. Summary

In these proceedings, we briefly summarize our recent study on the baryonic spin Hall effect (SHE) for the local Lambda spin polarization. Based on MUSIC simulations with AMPT initial condition and spin Cooper–Fryer on the freeze-out surface, we found the baryonic SHE shows a sizeable effect on $P_z(\phi)$ and $P_y(\phi)$ at RHIC BES energies, which leads to the local polarization separation between baryons and anti-baryons at 7.7 GeV. To isolate the baryonic SHE contribution, we predict the second Fourier coefficients of net spin polarization in the longitudinal and transverse directions, which show non-trivial collision energy dependence and can be used as possible signals to detect baryonic SHE in future experiments.

This work was supported in part by the NSFC under grants No. 12075007, No. 11675004 (B.F. and H.S.), No. 12147173 (B.F.), No. 11861131009 and No. 12075098 (L.P.). Y.Y. thanks for the support from the Strategic Priority Research Program of the Chinese Academy of Sciences, grant No. XDB3400 0000. We also acknowledge the extensive computing resources provided by the Supercomputing Center of the Chinese Academy of Science (SCCAS), Tianhe-1A from the National Supercomputing Center in Tianjin, China, and the High-performance Computing Platform of the Peking University.

REFERENCES

- [1] Zuo-Tang Liang, Xin-Nian Wang, *Phys. Rev. Lett.* **94**, 102301 (2005); *Erratum ibid.* **96**, 039901 (2006).
- [2] Zuo-Tang Liang, Xin-Nian Wang, *Phys. Lett. B* **629**, 20 (2005).
- [3] F. Becattini, V. Chandra, L. Del Zanna, E. Grossi, *Ann. Phys.* **338**, 32 (2013).

- [4] F. Becattini, Iu. Karpenko, *Phys. Rev. Lett.* **120**, 012302 (2018).
- [5] Baochi Fu, Kai Xu, Xu-Guang Huang, Huichao Song, *Phys. Rev. C* **103**, 024903 (2021).
- [6] Xiao-Liang Xia, Hui Li, Ze-Bo Tang, Qun Wang, *Phys. Rev. C* **98**, 024905 (2018).
- [7] De-Xian Wei, Wei-Tian Deng, Xu-Guang Huang, *Phys. Rev. C* **99**, 014905 (2019).
- [8] Shuai Y.F. Liu, Yi Yin, *J. High Energy Phys.* **2107**, 188 (2021).
- [9] Baochi Fu, Shuai Y.F. Liu, Longgang Pang, Huichao Song, Yi Yin, *Phys. Rev. Lett.* **127**, 142301 (2021).
- [10] F. Becattini, M. Buzzegoli, A. Palermo, *Phys. Lett. B* **820**, 136519 (2021).
- [11] F. Becattini *et al.*, *Phys. Rev. Lett.* **127**, 272302 (2021).
- [12] Dam Thanh Son, Naoki Yamamoto, *Phys. Rev. D* **87**, 085016 (2013).
- [13] Yoshimasa Hidaka, Shi Pu, Di-Lun Yang, *Phys. Rev. D* **95**, 091901 (2017).
- [14] Yoshimasa Hidaka, Shi Pu, Di-Lun Yang, *Phys. Rev. D* **97**, 016004 (2018).
- [15] Koichi Hattori, Yoshimasa Hidaka, Di-Lun Yang, *Phys. Rev. D* **100**, 096011 (2019).
- [16] Cong Yi, Shi Pu, Di-Lun Yang, *Phys. Rev. C* **104**, 064901 (2021).
- [17] Baochi Fu, Longgang Pang, Huichao Song, Yi Yin, [arXiv:2201.12970](https://arxiv.org/abs/2201.12970) [hep-ph].
- [18] Shuai Y. F. Liu, Yi Yin, *Phys. Rev. D* **104**, 054043 (2021).
- [19] Sangwook Ryu, Vahidin Jupic, Chun Shen, *Phys. Rev. C* **104**, 054908 (2021).
- [20] W. Florkowski, A. Kumar, A. Mazeliauskas, R. Ryblewski, *Phys. Rev. C* **105**, 064901 (2021).
- [21] Yifeng Sun, Zhen Zhang, Che Ming Ko, Wenbin Zhao, *Phys. Rev. C* **105**, 034911 (2022).
- [22] Sahr Alzhrani, Sangwook Ryu, Chun Shen, *Phys. Rev. C* **106**, 014905 (2022).
- [23] Björn Schenke, Sangyong Jeon, Charles Gale, *Phys. Rev. C* **82**, 014903 (2010).
- [24] Zi-Wei Lin, Che Ming Ko, Bao-An Li, Bin Zhang, Subrata Pal, *Phys. Rev. C* **72**, 064901 (2005).
- [25] Hao-jie Xu, Zhuopeng Li, Huichao Song, *Phys. Rev. C* **93**, 064905 (2016).